Bright stationary solitary waves in deep gratings with a quadratic nonlinearity

Awdah Arraf,[1,2,*] C. Martijn de Sterke,[1,2] and H. He[1]
[1]*School of Physics, University of Sydney, NSW 2006, Australia*
[2]*Australian Photonics Cooperative Research Centre, Australian Technology Park, Eveleigh, NSW 1430, Australia*
(Received 9 September 1999; revised manuscript received 17 October 2000; published 26 January 2001)

We present localized, bright, stationary soliton solutions to the coupled-mode equations for quadratically nonlinear media with a *deep* grating. We find that the required peak intensities can be significantly lower than might be expected from a shallow grating treatment.

DOI: 10.1103/PhysRevE.63.026611 PACS number(s): 42.65.Tg, 42.65.Ky

I. INTRODUCTION

Periodic Kerr media are well known to support Bragg solitons, which maintain their shape through the balance of the grating's group velocity dispersion and the Kerr nonlinearity [1]. It is also well known that in second harmonic generation (SHG), the up and down conversion between the fundamental frequency (FF) and the second harmonic frequency (SHF), can lead to a nonlinear phase shift somewhat similar to that in Kerr media, but potentially much larger [2,3]. One would thus expect $\chi^{(2)}$ media with a periodic refractive index to support solutions that are similar to Bragg solitons. Indeed, this was confirmed theoretically [4–9]. Here we theoretically investigate such solitons further, without making the usual assumption that the grating is a weak perturbation.

The usual starting point for studies of gratings with a quadratic nonlinearity is a set of four coupled-mode equations (CMEs). For shallow gratings, these are well established and many solutions are known [5–9]. The CMEs for deep gratings are also known and include additional nonlinear terms [10], though their solutions were only considered in limiting cases [5,6]. In this paper we present stationary soliton solutions for $\chi^{(2)}$ media with a deep grating. We compare the results to those for shallow gratings [6–9], and show that the peak intensities according to the deep grating treatment can be significantly lower than might be expected from the usual method.

II. COUPLED-MODE EQUATIONS

We consider scalar type I SHG in which the FF is $\omega_{10}+\gamma$, where ω_{10} is the center of the first grating-induced band gap. Through the $\chi^{(2)}$ nonlinearity, this field generates the SHF near the center of the second band gap ω_{20}; because of dispersion, $\omega_{20}-2\omega_{10}\neq 0$. Here and below, the subscript $m=1,2$, refers to the FF and the SHF or the first and the second band gaps. We restrict ourselves to envelopes varying harmonically in time. According to Arraf and de Sterke [10] these obey

$$
\begin{aligned}
&+i\mathcal{E}'_{1+}+\frac{\gamma}{v_{1g}}\mathcal{E}_{1+}+\kappa_1\mathcal{E}_{1-}+\Gamma_1\mathcal{E}^*_{1+}\mathcal{E}_{2+}\\
&+\Gamma_2\mathcal{E}^*_{1+}\mathcal{E}_{2-}+\Gamma_3\mathcal{E}^*_{1-}\mathcal{E}_{2+}+\Gamma^*_3\mathcal{E}^*_{1-}\mathcal{E}_{2-}=0,\\
&+i\mathcal{E}'_{2+}+\frac{2\gamma}{v_{2g}}\mathcal{E}_{2+}+\delta k\mathcal{E}_{2+}+\kappa_2\mathcal{E}_{2-}+\Gamma^*_1\mathcal{E}^2_{1+}\\
&+\Gamma_2\mathcal{E}^2_{1-}+2\Gamma^*_3\mathcal{E}_{1+}\mathcal{E}_{1-}=0,
\end{aligned}
\tag{1}
$$

where $\mathcal{E}_{\pm}$ are the envelopes associated with forward and backward propagation, and the prime ($'$) indicates differentiation with respect to the propagation direction z. As discussed below, the evolution equations for the $\mathcal{E}_-$ are not required here. The positive, real constants κ_m are grating coupling constants, v_{mg} are the group velocities, $\delta k=k_2-2k_1$, where the k_m are the wave numbers at the FF and the SHF, and the complex nonlinear coefficients Γ_{1-3} are known [10].

The dispersion relation in Fig. 1 is obtained by substituting trial plane wave solutions into the linear part of Eqs. (1), taking $v_{1g}=v_{2g}=v_g$ (see below). The first band gap (left-hand side) is centered at $\gamma=0$, while the second band gap (right-hand side) is centered at $\gamma=-v_g\delta k/2$. In the linear limit, an envelope $\mathcal{E}_{m\pm}(z)$ tuned to a frequency within a band gap is evanescent, while otherwise it is oscillatory.

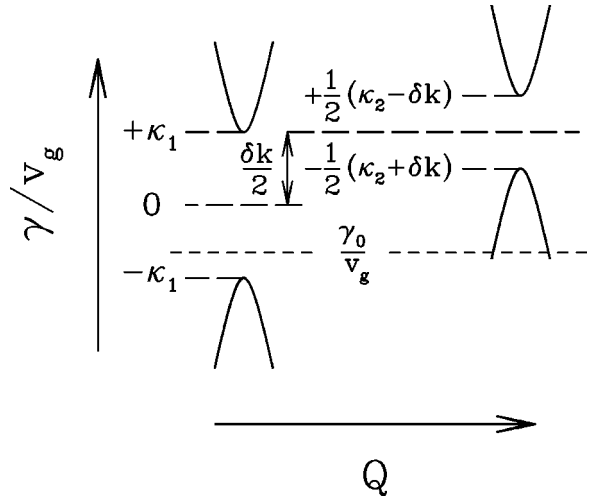

FIG. 1. Schematic of the dispersion relation showing the local detuning γ/v_g versus the local wave number Q.

*Electronic address: a.arraf@physics.usyd.edu.au

Equations (1) apply to arbitrary periodic refractive index. Henceforth however, we consider refractive indices that are symmetric around the center of each period. The Γ's in Eqs. (1) are then either real (regime I) or imaginary (regime II) but never complex [10].

In the stationary limit that we consider here $\mathcal{E}_{m-}=\mathcal{E}_{m+}^{\star}$, and so only two of Eqs. (1) are required. Rather, by writing [9] $\mathcal{E}_{m\pm}(z)=\sqrt{m/2}[p_m(z)\pm iq_m(z)]$, where p_m and q_m are real, they reduce to four real equations. This leads to a Hamiltonian system, which in regime I reads

$$\begin{aligned} q_1' &= K_{1+}p_1+\varphi_+p_1p_2+\varphi_0q_1q_2,\\ p_1' &= K_{1-}q_1+\varphi_-q_1p_2-\varphi_0p_1q_2,\\ q_2' &= K_{2+}p_2+\frac{\varphi_+}{2}p_1^2-\frac{\varphi_-}{2}q_1^2,\\ p_2' &= K_{2-}q_2-\varphi_0p_1q_1, \end{aligned} \tag{2}$$

where the $\varphi_{0,\pm}$ are combinations of the Γ_{1-3}

$$\varphi_0=\Gamma_1-\Gamma_2,\quad \varphi_\pm=\Gamma_1+\Gamma_2\pm 2\Gamma_3, \tag{3}$$

and where $K_{m\pm}$ are given by

$$K_{1\pm}=\kappa_1\pm\frac{\gamma}{v_{1g}},\quad K_{2\pm}=\kappa_2\pm\left(\delta k+\frac{2\gamma}{v_{2g}}\right). \tag{4}$$

Results for regime II are similar. Henceforth we take $v_{1g}=v_{2g}=v_g$. Note that for GaAs at a fundamental wavelength of 1.6 μm, $v_{2g}/v_{1g}=0.92$, while for AlAs, $v_{2g}/v_{1g}=0.93$ [12], so this is a good approximation.

Equations (2) can be solved analytically in the cascading limit when the dispersion is large, i.e., $|\delta k|\gg\kappa_m$ [4,6]. The conversion from the FF into the SHF is then inefficient and $p_1(z),q_1(z)\gg p_2(z),q_2(z)$. In the last two of Eqs. (2) the δk term [in the $K_\pm$ in Eqs. (4)] and the nonlinear terms now dominate, and thus $p_2=-(\varphi_+p_1^2-\varphi_-q_1^2)/(2\delta k)$ and $q_2=-\varphi_0p_1q_1/\delta k$, so that the SHF is slaved by the FF. Substituting into the first two of Eqs. (2) we find

$$\begin{aligned} q_1' &= K_{1+}p_1-\varphi_{s+}p_1^3-\varphi_{s0}q_1^2p_1,\\ p_1' &= K_{1-}q_1+\varphi_{s-}q_1^3+\varphi_{s0}q_1p_1^2, \end{aligned} \tag{5}$$

where

$$\varphi_{s\pm}=\varphi_\pm^2/(2\delta k), \tag{6}$$

$$\varphi_{s0}=(2\varphi_0^2-\varphi_+\varphi_-)/(2\delta k). \tag{7}$$

Equations (5) are similar to those of de Sterke *et al.* [11], who considered deep gratings with a Kerr nonlinearity. This is not surprising since in the cascading limit a $\chi^{(2)}$ acts as a $\chi^{(3)}$ effect.

Equations (5) have the solutions [11,13]

$$p_1=-\sqrt{2K_{1+}/N}\,\alpha\sinh(\alpha z), \tag{8}$$

$$q_1=+\sqrt{2K_{1-}/N}\,\alpha\cosh(\alpha z), \tag{9}$$

where

$$\begin{aligned} N=\varphi_{s+}K_{1-}^2\cosh^4(\alpha z)+2\varphi_{s0}K_{1+}K_{1-}\\ \times\cosh^2(\alpha z)\sinh^2(\alpha z)+\varphi_{s-}K_{1+}^2\sinh^4(\alpha z) \end{aligned} \tag{10}$$

with $\alpha=(K_{1+}K_{1-})^{1/2}$ and where $\delta k>0$. For $\delta k<0$ the hyperbolic sine and cosine functions interchange.

III. RESULTS

The shallow grating CMEs have two types of bright solutions [6,7,14]. In the first, both the FF and the SHF are tuned inside their linear band gaps (free tail solutions [14]). In the low-intensity wings, therefore, the free envelopes are evanescent. In the second, the SHF is outside its band gap (locked tail solutions [14]). Though the free linear SHF solutions are thus propagating, the SHF–FF coupling forces the SHF field to decay in the wings.

Free tail and locked tail solutions differ in applying initial conditions [6–9]. We start integrating in one of the soliton wings, on a small hypersphere of radius r, i.e.,

$$p_1^2+q_1^2+2(p_2^2+q_2^2)=r^2, \tag{11}$$

where analytic expressions can be found. For locked tail solutions, the initial conditions are now specified by requiring that the soliton decays in the other wing. However, for free tail solutions, one of the initial conditions is as yet unspecified and is found using a shooting method.

The *nonlinear* parameters used apply to a GaAs–AlAs stack. For wavelengths $\lambda_{\rm FF}=1.6$ μm and $\lambda_{\rm SHF}=0.8$ μm, the refractive indices are $n_{1\rm GaAs}=3.37$, $n_{1\rm AlAs}=2.88$, $n_{2\rm GaAs}=3.67$, and $n_{2\rm AlAs}=3.04$ [12]. Following Miller's rule, we take the $\chi^{(2)}$ ratio between AlAs and GaAs to be 0.33 [15]. We use $d_{\rm GaAs}/d=0.19$, where $d_{\rm GaAs}/d$ is the GaAs fraction of the period. Treating this grating as if it was shallow, the Bloch functions are simple trigonometric functions which, using the definitions of the Γ's [10], leads to $\Gamma_2=\Gamma_3=0$, and only $\Gamma_1=\Gamma_1^{\rm sh}\neq 0$. The full deep grating treatment requires the exact Bloch functions [10], corresponding to a Fourier series, and which exhibit discontinuous derivatives at the interfaces. Using these Bloch functions, we then similarly find $\Gamma_1=0.85\Gamma_1^{\rm sh}$, $\Gamma_2=0.15\Gamma_1^{\rm sh}$, and $\Gamma_3=0.17\Gamma_1^{\rm sh}$. Below we use units in which $\Gamma_1^{\rm sh}=1$. We note that for $d_{\rm GaAs}/d=0.19$ the difference between the shallow and deep grating treatments are the most pronounced.

Though the nonlinear coefficients apply to GaAlAs, the *linear* coefficients are independent of this geometry. We first take $v_g\kappa_1=1.0$, $v_g\kappa_2=0.5$, and $\gamma_0=-0.9v_g$, so that the FF lies just above the bottom edge of the band gap (see Fig. 1). We then vary δk between $\pm\infty$ so that the SHF lies in one of three regions RI, RII, and RIII, depending on whether it is above, inside, or below its band gap, respectively, where, according to Fig. 1,

$$\text{RI:}\ -(\kappa_2+2\gamma_0/v_g)\leqslant\delta k<+\infty,$$

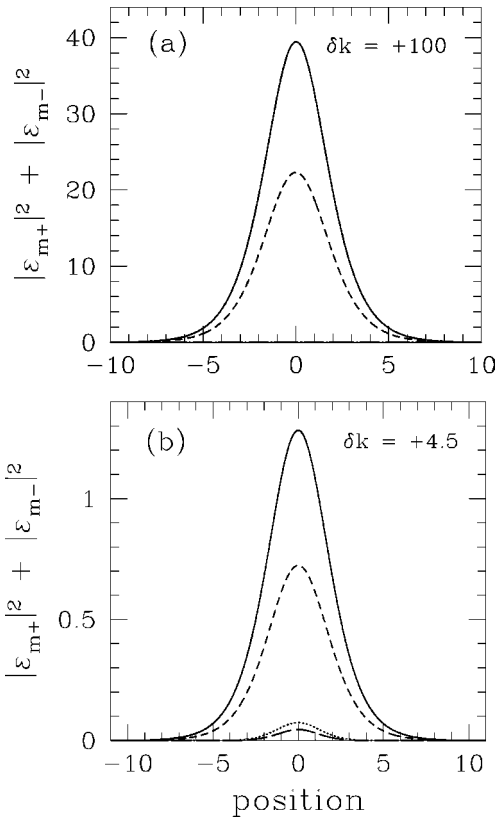

FIG. 2. Soliton solutions in RI, showing $|\mathcal{E}_{m+}|^2+|\mathcal{E}_{m-}|^2$ versus position. The short-dashed and long-dashed curves are deep grating results for the FF and SHF, respectively. The solid and dotted curves are the same, but in the shallow grating approximation.

$$\text{RII:} +(\kappa_2-2\gamma_0/v_g)<\delta k<-(\kappa_2+2\gamma_0/v_g), \qquad (12)$$

$$\text{RIII:} -\infty<\delta k\leqslant+(\kappa_2-2\gamma_0/v_g).$$

For our geometry, the boundaries between RI, RII, and RIII are at $\delta k=+2.3v_g$ and $\delta k=+1.3v_g$. Soliton solutions are shown in Figs. 2 and 3 for RI and RII, respectively, all with $r=10^{-6}$ in Eq. (11). No results are shown for RIII as all are found to be unstable.

In Fig. 2(a) we have $\delta k=+100v_g$, and the SHF thus lies far above the second band gap. Note that, apart from the value of the peak intensity, the deep and shallow grating solutions are very similar. Since $|\delta k|\gg\kappa_m$ we expect the cascading results to apply. According to Eqs. (8) the peak intensity is

$$|\mathcal{E}_{1+}|^2+|\mathcal{E}_{1-}|^2=\frac{2K_{1+}}{\varphi_{s+}}\equiv\frac{4\delta kK_{1+}}{(\Gamma_1+\Gamma_2+2\Gamma_3)^2}, \qquad (13)$$

in agreement with the numerical result, from which they cannot be distinguished on this scale. Thus the shallow grating treatment underestimates the effect of the nonlinearity, since the nonlinear coefficients in (13) add. To check stability, the fully time-dependent CMEs [Eqs. (22) in Ref. [10]] were solved numerically using a finite difference scheme [16]. The solutions in Figs. 2(a) were found to be robust in at least two independent runs of 2500 time units, corresponding to roughly 5 ns for the AlGaAs structures that we are considering, against additional, random Gaussian noise with a strength of 1% of the peak intensity. The noise was applied independently to the real and imaginary parts of $\mathcal{E}_{m\pm}$. This implies that the solutions are stable. Shallow grating results were checked independently [17]. The stability of solutions presented below are checked similarly. We note that gap solitons that occur in gratings with a $\chi^{(3)}$ nonlinearity have been shown to exhibit oscillatory instabilities [18], which may be difficult to observe using a direct numerical calculation.

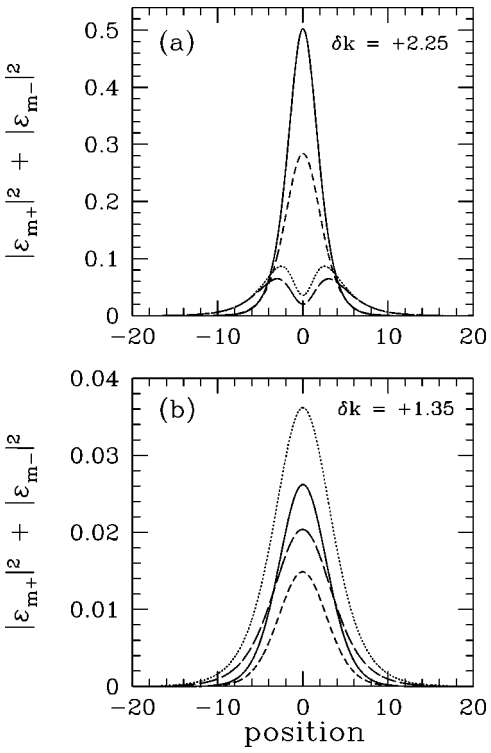

FIG. 3. The same as Fig. 2, but for RII.

As δk decreases the SHF starts to approach the second band gap at $\delta k=2.3v_g$ and the peak intensity decreases. This is illustrated in Fig. 2(b), which shows solutions for $\delta k=+4.5v_g$. Again, both solutions are stable and the deep grating intensity is more than three times smaller than the shallow grating result. For smaller δk, but still in RI, we find that when $3.6v_g\leqslant\delta k\leqslant+\infty$, the solutions are similar to Fig. 2, and that all are stable; no soliton solutions are found for $+2.3v_g\leqslant\delta k\leqslant+3.6v_g$. In the shallow grating approximation no solutions are found for $+2.3v_g\leqslant\delta k\leqslant+3.1v_g$.

Reducing δk further tunes the SHF into the second band gap and we enter RII. Figure 3(a) shows solutions for $\delta k=+2.25v_g$ where the SHF lies just below the upper band edge. The FF component is single peaked while the SHF component has a double peak. In Fig. 3(b), $\delta=1.35v_g$, so that the SHF is tuned just above the lower band edge. All solutions shown in Fig. 3 are stable. Since δk in this region is small the peak intensities are much lower than in RI (Fig. 2). We find again that in RII the deep grating and shallow grating solutions are similar, but that the deep grating solutions again have peak intensities roughly half that for shallow gratings.

IV. DISCUSSION AND CONCLUSIONS

Although the results in Sec. III are for $v_g\kappa_1=1.0$, $v_g\kappa_2=0.5$, and $\gamma_0=-0.9v_g$, other geometries and detunings were also considered. Here we discuss these cases briefly. Results for $\kappa_2\neq\kappa_1/2$ are broadly similar to those in Sec. III. For $\gamma_0=+0.9v_g$ the results are also similar to those in Sec. III, except that RI and RIII are interchanged. More generally, for $\gamma<0$ the trends are similar to those for $\gamma_0=-0.9v_g$, whereas if $\gamma_0>0$ they are similar to those for $\gamma_0=+0.9v_g$.

We now consider regime II. Recall that for shallow gratings, changing the sign of κ_2 corresponds to changing between regimes I and II. Since the shallow grating equations are unchanged under the transformation

$$\gamma_0\rightarrow-\gamma_0,\quad \delta k\rightarrow-\delta k,\quad \kappa_2\rightarrow-\kappa_2,$$
$$p_1\rightarrow q_1,\quad q_1\rightarrow p_1,\quad q_2\rightarrow-q_2,\quad p_2\rightarrow p_2, \tag{14}$$

solutions obtained in regime I for γ_0 and δk are the same as those for regime II with the FF tuned to $-\gamma_0$ and $-\delta k$. Thus, soliton solutions calculated for $\gamma_0=\mp0.9v_g$ in regime I are identical to those for the same $v_g\kappa_m$ with $\gamma_0=\pm0.9v_g$ in regime II. Although (14) is only valid for shallow gratings we find that the results using the deep grating treatment follow the same trend.

Almost all previous work in this area applies to shallow gratings [4–9]. We did compare our results with previous work in this limit, particularly that of Conti *et al.* [6] and Peschel *et al.* [8], and find identical results. Deep grating work includes that of Conti *et al.*, who use a Bloch function approach to derive two coupled nonlinear Schrödinger equations [5]. These were shown to support bright solitary waves with a hyperbolic secant profile [5]. Conti *et. al.* [6] applied an approach similar to ours, but they took the shallow grating limit before calculating the nonlinear coefficients and found $\Gamma_{2,3}=0$.

The stability of gap solitons in the cascading limit was analyzed by Conti *et al.* [7]. They found that all stationary solutions are stable, in contradiction to our findings, according to which for $\gamma=-0.9\kappa$ and $\delta k<0$, all solutions are unstable. However, we consider the full CMEs, whereas Conti *et al.* [7] used the modified CMEs in the cascading limit. We also numerically analyzed the stability in this limit using Eqs. (5), and find the solutions in RIII to be stable, in agreement with Conti *et al.* [7]. Apparently the relevant instability mechanism is dropped in taking the cascading limit. In more recent work [6] Conti *et al.* note that in the cascading limit only the solutions for $\delta k>0$ are stable, consistent with our findings.

In conclusion, we consider localized, bright, stationary solitons in deep gratings with a quadratic nonlinearity. By varying the material dispersion we find solutions for which the SHF is tuned above, within and below the second gap. We can of course not vary δk freely. However the relevant parameters in the normalized CMEs are $\delta k/\kappa_m$, which, in effect, can be tuned by varying κ_1 and κ_2 [9]. In the cascading limit analytic solutions to the CMEs are given. Using the full time-dependent CMEs we checked the stability of all solutions. We find that results of the deep grating treatment are similar to those from the shallow grating approximation, except that the former indicates peak intensities that are roughly a factor of 2 smaller than the latter. Though this can be understood quantitatively in the cascading limit, it appears to hold for a wide range of parameters. For the examples given here, that are not optimized in any way, the soliton's peak power is around 100 GW/cm^2. It is well known, however, that the power required to launch such a soliton may be substantially lower than the peak power inside the structure [19].

ACKNOWLEDGMENTS

This work is supported by the Australian Research Council.

[1] B. J. Eggleton, R. E. Slusher, C. M. de Sterke, P. A. Krug, and J. E. Sipe, Phys. Rev. Lett. **76**, 1627 (1996).
[2] Y. N. Karamzin and A. P. Sukhorukov, Zh. Eksp. Teor. Fiz. **68**, 834 (1975) [Sov. Phys. JETP **41**, 414 (1976)].
[3] W. E. Torruellas, Z. Wang, D. J. Hagan, E. W. VanStryland, G. I. Stegeman, L. Torner, and C. R. Menyuk, Phys. Rev. Lett. **74**, 5036 (1995).
[4] Y. S. Kivshar, Phys. Rev. E **51**, 1613 (1995).
[5] C. Conti, S. Trillo, and G. Assanto, Opt. Lett. **22**, 1350 (1997); Phys. Rev. Lett. **78**, 2341 (1997); Opt. Lett. **22**, 445 (1997).
[6] C. Conti, S. Trillo, and G. Assanto, Opt. Lett. **23**, 334 (1998); Phys. Rev. E **57**, R1251 (1998); Opt. Exp. **3**, 389 (1998); Phys. Rev. E **59**, 2467 (1999).
[7] C. Conti, A. De Rossi, and S. Trillo, Opt. Lett. **23**, 1265 (1998).
[8] T. Peschel, U. Peschel, F. Lederer, and B. A. Malomed, Phys. Rev. E **55**, 4730 (1997).
[9] H. He and P. D. Drummond, Phys. Rev. Lett. **78**, 4311 (1997); Phys. Rev. E **58**, 5025 (1998).
[10] A. Arraf and C. M. de Sterke, Phys. Rev. E **58**, 7951 (1998).
[11] C. M. de Sterke, D. G. Salinas, and J. E. Sipe, Phys. Rev. E **54**, 1969 (1996).
[12] H. C. Casey, Jr. and M. B. Panish, *Heterostructure Laser* (Academic, New York, 1978).
[13] Y. S. Kivshar and N. Flytzanis, Phys. Rev. A **46**, 7972 (1992).
[14] W. C. K. Mak, B. A. Malomed, and P. L. Chu, Phys. Rev. E **58**, 6708 (1998).
[15] R. W. Boyd, *Nonlinear Optics* (Academic, San Diego, 1992).
[16] C. M. de Sterke, K. R. Jackson, and B. D. Robert, J. Opt. Soc. Am. B **8**, 403 (1991).
[17] P. D. Drummond and I. K. Mortimer, J. Comput. Phys. **93**, 144 (1991).
[18] A. D. Rossi, C. Conti, and S. Trillo, Phys. Rev. Lett. **81**, 85 (1998).
[19] B. J. Eggleton, C. M. de Sterke, and R. E. Slusher, J. Opt. Soc. Am. B **16**, 587 (1999).